Steel and Composite Structures, *Vol. 22, No. 5 (2016) 1193-1214*
DOI: http://dx.doi.org/10.12989/scs.2016.22.5.1193

Three-dimensional stresses analysis in rotating thin laminated composite cylindrical shells

Isa Ahmadi * and Mahsa Najafi [a]

Advanced Materials and Computational Mechanics Lab., Department of Mechanical Engineering, University of Zanjan, University Blvd, P.O Box 45371-38791, Zanjan, Iran

(*Received May 17, 2016, Revised November 07, 2016, Accepted November 15, 2016*)

Abstract. In this paper, the 3D stress state and inter-laminar stresses in a rotating thin laminated cylinder shell are studied. The thickness of the cylinder is supposed to be thin and it is made of laminated composite material and can have general layer stacking. The governing equations of the cylindrical shell are obtained by employing the Layerwise theory (LWT). The effect of rotation is considered as rotational body force which is induced due to the rotation of the cylinder about its axis. The Layerwise theory (LWT), is used to discrete the partial differential equations of the problem to ordinary ones, in terms of the displacements of the mathematical layers. By applying the Free boundary conditions the solution of the governing equations is completed and the stress state, the inter-laminar stresses, and the edge effect in the rotating cylindrical shells are investigated in the numerical results. To verify the results, LWT solution is compared with the results of the FEM solution and good agreements are achieved. The inter-laminar normal and shear stresses in rotating cylinder are studied and effects of layer stacking and angular velocity is investigated in the numerical results.

Keywords: rotating cylindrical shell; inter-laminar stresses; layerwise theory; laminated composite

1. Introduction

Composite structures are widely used in engineering fields such as aerospace, submarine, automotive, and other applications, due to their light weight, excellent mechanical properties, high energy absorption, high stiffness to weight, and high strength to weight ratio. Because of mentioned mechanical properties of the composite structures several studies are presented at this field. (Madhukar and Singha 2013, Mantari *et al*. 2012, Varadan and Bhaskar 1991, Kapoor *et al*. 2013).

Beside the advantageous of composite materials, delamination is one of the most important problems in the application of the composite structures that is caused by three dimensional stress states, especially the inter-laminar stresses in the vicinity of the edges. So, Inter-laminar stresses are particularly important in causing failure of structural components, which are made of composite materials. The reason is that they are significantly contributed to various damages such as delamination phenomenon as stated. According to mentioned facts, inter-laminar stresses at the

∗Corresponding author, Assistant Professor, E-mail: i_ahmadi@znu.ac.ir
[a] Ph.D. Student, E-mail: MahsaNajafi@znu.ac.ir

 ISSN: 1229-9367 (Print), 1598-6233 (Online)

free edges (where the Classical Laminated Theory (CLT) is invalid) are considered in various researches.

Hayashi (1967) and Puppo and Evensen (1970) studied inter-laminar shear stresses near the free edge of laminated composite structures. Because of the plane stress, their model refused the existence of the normal inter-laminar stress. Whitney (1973) presented a review of free edge effect in laminated plates. Byron Pipes and Pagano (1974) used an elasticity solution to calculate inter-laminar stresses in symmetric layers. Pagano (1974) also used a higher order theory to study inter-laminar stresses. An analytical boundary layer theory was used by Levy and Tang (1975) to predict inter-laminar stresses at the vicinity of the free edge of asymmetric laminated composite under non-axial tension.

Waltz and Vinson (1976) studied inter-laminar stresses in circular laminated cylindrical shells subjected to internal pressure by using elastic shell theory. They have shown that the amount of inter-laminar stresses are maximum at the edges and claimed that in the case of high inter-laminar stresses delamination can happen at this region. Various investigations are conducted to composite structures, by using numerous theories and approaches like the CLT and the first order shear deformation theory. It should be mentioned that, as there are differences in the material properties of lamina in the laminates, a theory which considers independent degrees of freedom, is required to study the inter-laminar stresses. So, to study the inter-laminar stresses Reddy (1992) presented LWST (Layerwise shell theory) which is widely used to this respect. Kassapoglou and Lagace (1986) analyzed inter-laminar stresses in symmetric laminated composites under non-axial tension. They (Kassapoglou and Lagace 1986) also used equilibrium of forces to study inter-laminar stresses in symmetric composites under torsion. Wu and Chi (1999) used a refined asymptotic theory to study inter-laminar stresses in the laminated composite shallow shells. Inter-laminar stresses analysis of a cylindrical shell under pressure is presented by Wang *et al*. (2002) using the elasticity solution. Başar *et al*. (2000) developed a multi-layer shell elements approach to analyze the inter-laminar stresses in the composite laminates. First, they presented a multi-director shell theory which was on the basis of quadratic approximation of the displacement field. Then they used Euler-angles and the single layer theory, which the latter was coupled with multi-layer concept that could accurately predict the complex-through thickness stress distribution. A higher-order Layerwise theory is used by Plagianakos and Saravanos (2009) for determination of inter-laminar stresses in thick laminated composite and sandwich plates. Asgari and Akhlaghi (2011) analyzed thick hollow cylinder using three dimensional elasticity solution. Layerwise theory also was used to study functionally graded (FG) cylindrical shell under dynamic load by Yas *et al*. (2011), thermal and mechanical loadings by Matsunaga (2009). Hosseini Kordkheili and Naghdabadi (2007) analyzed stresses and displacements of FGM cylindrical shells under thermal and mechanical loading. Afshin *et al*. (2010) studied inter-laminar stresses in laminated composite sheets and cylindrical sandwich panels with flexible core by using Layerwise theory (LWT). Miri and Nosier (2011) studied edge effect in cross-ply laminated circular shell panels by two solutions: Reddy's Layerwise theory and the stress-function approach along with Fourier series. Vijayakumar (2011) studied inter-laminar stresses in symmetric laminated composite plates with isotropic plies under bending load. Yang *et al*. (2013) presented a combination of the first shear theory and Layerwise theory to compute inter-laminar stresses in a laminated composite plate subjected to uniform load. They studied the effect of the ply angle on the shapes of stresses. Ealias *et al*. (2013) studied the edge effect in composite structures. Maturi *et al*. (2014) presented a LWT (using collocation and radial basis functions) to analyze inter-laminar stresses within the interfaces of sandwich plates. Khandelwal and Chakrabarti (2015) used a refined higher order theory to

determine the inter-laminar stresses in the laminated shallow shells. Edfawy (2016) studied the transient thermal stresses in a non-homogeneous orthotropic infinite cylinder. Alankaya and Oktem (2016) presented an analytical solution based on a third order shear deformation theory for the problem of static analysis of cross-ply doubly-curved shells and compared the results with the results of FE method. Javed *et al*. (2016) studied the free vibration behavior of non-uniform cylindrical shells using spline approximation under first order shear deformation theory. Four and two layered cylindrical shells and two different boundary conditions are analyzed. Ahmadi (2016) studied the edge interlaminar stresses in laminated panel which is subjected to extension force using LWT. Goswami and Becker (2016) studied inter-laminar stresses in sandwich plates considering three layers including a compressible core at the middle using LWT.

To the knowledge of the authors, analysis of the inter-laminar stresses and edge effect in the rotating composite cylinders is not found in the open literature. In this study, a laminated cylinder with finite length and general layer stacking which is subjected to rotational body force is investigated. It is well established that the single layer theories such as classical and first order shear deformation theory of plates and shells cannot relied on to predict the out of plane stress and local three dimensional stresses in the laminates. In this study, in order to study the inter-laminar stresses and local phenomena such as the edge effect in the rotating laminated cylinder, the LWT is employed. The LWT is used to discrete the partial differential equations to ordinary ones in terms of the displacement of mathematical layers. The ordinary differential equations are solved analytically and the inter-laminar stresses and the edge effect are studied in the current study. In order to study the accuracy of the results, the results of LWT solution and FEM solution for the rotating composite cylinder are compared. The convergence of the results with increasing the number of mathematical layers is studied. Various numerical results are presented to study the inter-laminar stresses distribution in cylinders with various layers stacking.

2. Governing equation

A laminated cylinder with general (arbitrary) layer stacking which is rotating with angular velocity of ω is considered. Based on the LWT, it is supposed that each physical layer in the laminated cylinder in the thickness consists of several imagined layers which are called numerical layers. N is the total number of numerical layers and $N+1$ is the total number of numerical surfaces

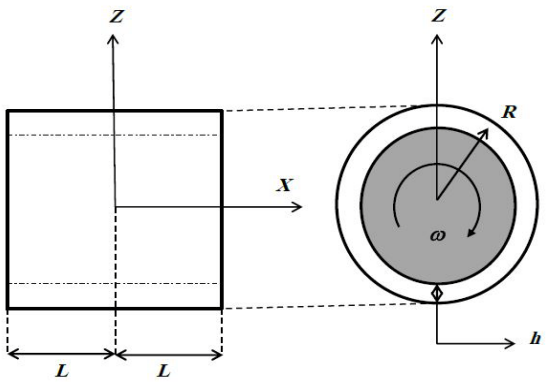

Fig. 1 The geometry of rotating laminated cylindrical shell

surfaces which includes interfaces of numerical layers, inner surface and outer surface of the cylinder. The cylindrical shell has a length of 2*L*, thickness *h*, mean radius of *R* and angular velocity of ω, which is shown in Fig. 1.

Due to the axisymmetric nature of the problem, it can be concluded that the displacement field (and stress field) in the cylinder does not depend on the angular coordinate θ of the cylinder and is a function of the length, *x*, and thickness, *z*-coordinate. So, according to the LWT of Reddy, the displacement components of a general point in the laminate can be assumed as

$$\begin{aligned} U(x,z) &= \sum_{i=1}^{N+1} u_i(x)\Phi_i(z) \\ V(x,z) &= \sum_{i=1}^{N+1} v_i(x)\Phi_i(z) \\ W(x,z) &= \sum_{i=1}^{N+1} w_i(x)\Phi_i(z) \end{aligned} \tag{1}$$

Where, $u_i(x)$, $v_i(x)$ and $w_i(x)$ are the displacements of *i-th* numerical surface in *x*, *y* and *z* directions. The Φ_i is a linear Lagrangian interpolation function, which has the unity value at the *i-th* interface and is equal to zero in the other ones. The linear Lagrangian interpolation function is defined as follows

$$\Phi_i = \begin{Bmatrix} 0 & z \le z_{i-1} \\ \psi_{i-1}^2 = \dfrac{z - z_{i-1}}{t_{i-1}} & z_{i-1} \le z \le z_i \\ \psi_i^1 = \dfrac{z_{i+1} - z}{t_i} & z_i \le z \le z_{i+1} \\ 0 & z \ge z_{i+1} \end{Bmatrix}, \qquad i = 1, 2, \ldots, N \tag{2}$$

Where $\psi_i^{1,2}$ (1 and 2 are superscript) are the Lagrange interpolation layer function or Lagrange interpolation local function of i-th layer (Kassegne and Reddy 1998) and t_i is the thickness of the *i*-th numerical layer. The repeated indexes represent the summation of indexes from 1 to $N + 1$. By substituting Eq. (1) into the strain-displacement relations, the strain components obtain as

$$\begin{aligned} \varepsilon_{xx} &= \frac{\partial U}{\partial x} = \frac{\partial u_i}{\partial x}\Phi_i \\ \varepsilon_{\theta\theta} &= \frac{\partial U}{\partial \theta} + \frac{W}{R} = \frac{w_j}{R}\Phi_i \\ \varepsilon_{zz} &= \frac{\partial W}{\partial z} = \frac{\partial \Phi_i}{\partial z} w_i \\ \gamma_{\theta x} &= \frac{\partial U}{\partial \theta} + \frac{\partial V}{\partial x} = \left(\frac{\partial v_i}{\partial x}\right)\Phi_i \end{aligned} \tag{3}$$

$$\gamma_{xz} = \frac{\partial U}{\partial z} + \frac{\partial W}{\partial x} = u_i \frac{\partial \Phi_i}{\partial z} + \frac{\partial w_i}{\partial x} \Phi_i$$
$$\gamma_{\theta z} = \frac{\partial V}{\partial z} + \frac{\partial W}{\partial \theta} - \frac{V}{R} = \left(-\frac{v_i}{R}\right) \Phi_i + v_i \frac{\partial \Phi_i}{\partial z} \tag{3}$$

Where $\psi_i^{1,2}$ (1 and 2 are superscript) are the Lagrange interpolation layer function or Lagrange interpolation local function of i-th layer (Kassegne and Reddy 1998) and t_i is the thickness of the *i*-th numerical layer. The repeated indexes represent the summation of indexes from 1 to $N+1$. By substituting Eq. (1) into the strain-displacement relations, the strain components obtain as

$$\pi\delta = \delta U + \delta V = 0 \tag{4}$$

Where $\psi_i^{1,2}$ (1 and 2 are superscript) are the Lagrange interpolation layer function or Lagrange interpolation local function of i-th layer (Kassegne and Reddy 1998) and t_i is the thickness of the *i*-th numerical layer. The repeated indexes represent the summation of indexes from 1 to $N + 1$. By substituting Eq. (1) into the strain-displacement relations, the strain components obtain as

$$\frac{\partial M_x^i}{\partial x} - Q_x^i = 0$$
$$\frac{\partial M_{x\theta}^i}{\partial x} - Q_\theta^i + \frac{1}{R} R_\theta^i = 0 \tag{5}$$
$$\frac{\partial R_x^i}{\partial x} - N_Z^i - \frac{1}{R} M_\theta^i + \rho R \omega^i = 0$$

Where in the above equations, the stress results are defined as

$$(M_x^i, R_\theta^i, M_{x\theta}^i) = \int_{\frac{-h}{2}}^{\frac{h}{2}} (\sigma_{xx}, \sigma_{xz}, \sigma_{x\theta}) \Phi_i \, dZ$$
$$(M_\theta^i, R_\theta^i) = \int_{\frac{-h}{2}}^{\frac{h}{2}} (\sigma_{\theta\theta}, \sigma_{\theta z}) \Phi_i \, dZ \tag{6}$$
$$(N_z^i, Q_\theta^i, Q_x^i) = \int_{\frac{-h}{2}}^{\frac{h}{2}} (\sigma_{zz}, \sigma_{\theta z}, \sigma_{xz}) \frac{d\Phi_i}{dz} dZ$$

And ω^i is defined as

$$\omega^i = \omega^2 \int_{\frac{-h}{2}}^{\frac{h}{2}} \Phi_i \, dz \tag{7}$$

$$\omega^i = \begin{cases} \dfrac{\omega^2 t_1}{2} & i = 1 \\ \dfrac{\omega^2 t_{i-1}}{2} + \dfrac{\omega^2 t_i}{2} & 1 < i < N+1 \\ \dfrac{\omega^2 t_N}{2} & i = N+1 \end{cases} \tag{8}$$

The strain-stress relation for the *i*-th numerical layer can be written as

$$\begin{Bmatrix} \sigma_{xx} \\ \sigma_{\theta\theta} \\ \sigma_{zz} \\ \sigma_{x\theta} \end{Bmatrix}^i = \begin{bmatrix} \bar{c}_{11} & \bar{c}_{12} & \bar{c}_{13} & \bar{c}_{16} \\ \bar{c}_{12} & \bar{c}_{22} & \bar{c}_{23} & \bar{c}_{26} \\ \bar{c}_{13} & \bar{c}_{23} & \bar{c}_{33} & \bar{c}_{36} \\ \bar{c}_{16} & \bar{c}_{26} & \bar{c}_{36} & \bar{c}_{66} \end{bmatrix}^i \begin{Bmatrix} \varepsilon_{xx} \\ \varepsilon_{\theta\theta} \\ \varepsilon_{zz} \\ \varepsilon_{x\theta} \end{Bmatrix}^i \qquad \begin{Bmatrix} \sigma_{\theta z} \\ \sigma_{xz} \end{Bmatrix}^i = \begin{bmatrix} \bar{c}_{44} & \bar{c}_{45} \\ \bar{c}_{45} & \bar{c}_{55} \end{bmatrix}^i \begin{Bmatrix} \varepsilon_{\theta z} \\ \varepsilon_{xz} \end{Bmatrix}^i \tag{9}$$

Where, $\{\sigma\}$ is the stress vector, $\{\varepsilon\}$ is the strain vector and $[\bar{C}]$ is the reduced mechanical stiffness matrix. Substituting aforementioned relations into Eq. (6), the stress resultants in terms of the displacements are obtained as

$$\begin{aligned} M_x^i &= D_{11}^{ij}\acute{u}_j + \frac{1}{R}D_{12}^{ij}w_j + D_{16}^{ij}\acute{v}_j + B_{13}^{ij}w_j \\ R_x^i &= B_{45}^{ij}v_j - \frac{1}{R}D_{45}^{ij}v_j + D_{55}^{ij}\acute{w}_j + B_{55}^{ij}u_j \\ M_{x\theta}^i &= D_{16}^{ij}\acute{u}_j + \frac{1}{R}D_{26}^{ij}w_j + B_{36}^{ij}w_j + D_{66}^{ij}\acute{v}_j \\ M_\theta^i &= D_{12}^{ij}\acute{u}_j + \frac{1}{R}D_{22}^{ij}w_j + B_{23}^{ij}w_j + D_{26}^{ij}\acute{v}_j \\ R_\theta^i &= B_{44}^{ij}v_j - \frac{1}{R}D_{44}^{ij}v_j + D_{45}^{ij}\acute{w}_j + B_{45}^{ij}u_j \\ N_z^i &= B_{13}^{ji}\acute{u}_j + \frac{1}{R}B_{23}^{ji}w_j + A_{33}^{ij}w_j + B_{36}^{ji}\acute{v}_j \\ Q_\theta^i &= \left(A_{44}^{ij} - \frac{1}{R}B_{44}^{ji}\right)v_j + B_{45}^{ji}\acute{w}_j + A_{45}^{ij}u_j \\ Q_x^i &= \left(A_{45}^{ij} - \frac{1}{R}B_{45}^{ji}\right)v_j + B_{55}^{ji}\acute{w}_j + A_{55}^{ij}u_j \end{aligned} \tag{10}$$

By substituting stress resultants into Eq. (5), the equations of motion are derived in terms of the displacements as

$$D_{11}^{ij}\frac{d^2u_j}{dx^2} + \left(\frac{1}{R}D_{12}^{ij} + B_{13}^{ij} - B_{55}^{ji}\right)\frac{dw_j}{dx} + D_{16}^{ij}\frac{d^2v_j}{dx^2} - \left(A_{45}^{ij} - \frac{1}{R}B_{45}^{ji}\right)v_j - A_{55}^{ij}u_j = 0 \tag{11}$$

$$
\begin{aligned}
&D_{16}^{ij}\frac{d^2u_j}{dx^2}-\left(B_{45}^{ji}-B_{45}^{ji}-\frac{1}{R}(D_{26}^{ij}+D_{45}^{ij})\right)\frac{dw_j}{dx}+D_{66}^{ij}\frac{d^2v_j}{dx^2}\\
&-\left(A_{44}^{ij}+\frac{1}{R^2}D_{44}^{ij}-\frac{1}{R}(B_{44}^{ij}+B_{44}^{ji})\right)v_j=0\\
&D_{55}^{ij}\frac{d^2w_j}{dx^2}-\left(B_{13}^{ji}-B_{55}^{ij}+\frac{1}{R}D_{12}^{ij}\right)\frac{du_j}{dx}-\left(B_{36}^{ji}+\frac{1}{R}(D_{26}^{ij}+D_{45}^{ij})-B_{45}^{ji}\right)\frac{dv_j}{dx}\\
&-\left(A_{33}^{ij}+\frac{1}{R^2}D_{22}^{ij}+\frac{1}{R}(B_{23}^{ij}+B_{23}^{ji})\right)w_j+\rho R\omega^i=0
\end{aligned}
\tag{11}
$$

Where the stiffness coefficients of laminates are defined as follows

$$
\begin{aligned}
A_{pq}^{i}&=\sum_{k=1}^{N}\int_{z_k}^{z_{k+1}}\bar{C}_{pq}^{(k)}\frac{d\Phi_i}{dz}dz\\
B_{pq}^{i}&=\sum_{k=1}^{N}\int_{z_k}^{z_{k+1}}\bar{C}_{pq}^{(k)}\Phi_i dz\\
A_{pq}^{ij}&=\sum_{k=1}^{N}\int_{z_k}^{z_{k+1}}\bar{C}_{pq}^{(k)}\frac{d\Phi_i}{dz}\frac{d\Phi_j}{dz}dz\\
B_{pq}^{ij}&=\sum_{k=1}^{N}\int_{z_k}^{z_{k+1}}\bar{C}_{pq}^{(k)}\Phi_i\frac{d\Phi_j}{dz}dz\\
D_{pq}^{ij}&=\sum_{k=1}^{N}\int_{z_k}^{z_{k+1}}\bar{C}_{pq}^{(k)}\Phi_i\Phi_j dz
\end{aligned}
\tag{12}
$$

where $i, j = 1, 2, \ldots N + 1$ and p, q can take values of 1, 2,…, 6. A_{pq}^{ij} and D_{pq}^{ij} are the symmetric matrices and B_{pq}^{ij} is not a symmetric matrix. By the integration of the above equations, the stiffness coefficients of laminates are derived as follows

$$
(A_{pq}^{ij},\ B_{pq}^{ij},D_{pq}^{ij})=
\begin{cases}
\left(-\dfrac{\bar{C}_{pq}^{(i-1)}}{t_{i-1}},-\dfrac{\bar{C}_{pq}^{(i-1)}}{2},\dfrac{t_{i-1}\bar{C}_{pq}^{(i-1)}}{6}\right) & j=i-1\\
\left(\dfrac{\bar{C}_{pq}^{(i-1)}}{t_{i-1}}+\dfrac{\bar{C}_{pq}^{(i)}}{t_i},\dfrac{\bar{C}_{pq}^{(i-1)}}{2}-\dfrac{\bar{C}_{pq}^{(i)}}{2},\dfrac{t_{i-1}\bar{C}_{pq}^{(i-1)}}{3}+\dfrac{t_i\bar{C}_{pq}^{(i)}}{3}\right) & j=i\\
\left(-\dfrac{\bar{C}_{pq}^{(i)}}{t_i},\dfrac{\bar{C}_{pq}^{(i)}}{2},\dfrac{t_i\bar{C}_{pq}^{(i)}}{6}\right) & j=i+1\\
(0,0,0) & j>i+1
\end{cases}
\tag{13}
$$

$$(A_{pq}^{i}, B_{pq}^{i}) =$$

$$\begin{cases} (-\bar{C}_{pq}^{(1)}, \dfrac{t_1 \bar{C}_{pq}^{(1)}}{2}) & i = 1 \\ (\bar{C}_{pq}^{(i-1)} - \bar{C}_{pq}^{(i)}, \dfrac{t_{i-1}\bar{C}_{pq}^{(i-1)}}{2} + \dfrac{t_i \bar{C}_{pq}^{(i)}}{2}) & 1 < i < N+1 \\ (\bar{C}_{pq}^{(N)}, \dfrac{t_N \bar{C}_{pq}^{(N)}}{2}) & i = N+1 \end{cases} \tag{14}$$

Due to the symmetry of the composite structure, the state-space variables are defined as follows

$$\{\eta\} = \begin{Bmatrix} \{U(x)\} \\ \{V(x)\} \\ \{W'(x)\} \end{Bmatrix}, \qquad \{\xi\} = \begin{Bmatrix} \{U'(x)\} \\ \{V'(x)\} \\ \{W(x)\} \end{Bmatrix} \tag{15}$$

In which for example $\{U\}$ is a column matrix and defined as

$$\{U\}^T = [U_1, U_2, \dots, U_{N+1}] \tag{16}$$

By substituting the conditional constrains into the equations of motion, following equations are obtained

$$\{\xi'\} = [A]\{\eta\}, \qquad \{\eta'\} = [B]\{\xi\} + \{f\} \tag{17}$$

Where $[A]$, $[B]$ and $\{f\}$ are defined by the equations of motion as follows

$$[A] = [A_1]^{-1}[A_2] \tag{18}$$

$$[B] = [B_1]^{-1}[B_2] \tag{19}$$

$$\{f\} = [B_1]^{-1} \begin{Bmatrix} 0 \\ 0 \\ -\rho R \omega^i \end{Bmatrix} \tag{20}$$

In which

$$[A_1] = \begin{bmatrix} D_{11}^{ij} & D_{16}^{ij} & 0 \\ D_{16}^{ij} & D_{66}^{ij} & 0 \\ 0 & 0 & I \end{bmatrix} \tag{21}$$

$$[A_2] = \begin{bmatrix} A_{55}^{ij} & A_{45}^{ij} - \dfrac{1}{R}B_{45}^{ji} & B_{55}^{ji} - \dfrac{1}{R}D_{12}^{ij} - B_{13}^{ij} \\ A_{45}^{ij} - \dfrac{1}{R}B_{45}^{ij} & A_{44}^{ij} + \dfrac{1}{R^2}D_{44}^{ij} - \dfrac{1}{R}(B_{44}^{ij} + B_{44}^{ji}) & B_{45}^{ji} - B_{45}^{ji} - \dfrac{1}{R}(D_{26}^{ij} + D_{45}^{ij}) \\ 0 & 0 & I \end{bmatrix} \tag{22}$$

And

$$[B_1] = \begin{bmatrix} 0 & 0 & D_{55}^{ij} \\ I & 0 & 0 \\ 0 & I & 0 \end{bmatrix} \tag{23}$$

$$[B_2] = \begin{bmatrix} B_{13}^{ji} - B_{55}^{ij} + \frac{1}{R} D_{12}^{ij} & B_{36}^{ji} + \frac{1}{R}(D_{26}^{ij} + D_{45}^{ij}) - B_{45}^{ji} & A_{33}^{ij} + \frac{1}{R^2} D_{22}^{ij} + \frac{1}{R}(B_{23}^{ij} + B_{23}^{ji}) \\ I & 0 & 0 \\ 0 & I & 0 \end{bmatrix} \tag{24}$$

It can be shown that the solution of Eq. (10) can be obtained as

$$\{\xi\} = [U][\cosh(\lambda x)]\{K_1\} + [U][\sinh(\lambda x)]\{K_2\} - [B]^{-1}\{F\} \tag{25}$$

$$\{\eta\} = [B][U][\Lambda]^{-1}[\sinh(\lambda x)]\{K_1\} + [B][U][\Lambda]^{-1}[\cosh(\lambda x)]\{K_2\} \tag{26}$$

Where $[\Lambda^2]$ is the eigenvalue and $[U]$ is the eigenvector of $[C] = [A]\,[B]$ as

$$[C][U] = [U][\Lambda^2] \tag{27}$$

And $\{K_1\}$ and $\{K_2\}$ are column matrix with $3(N + 1)$ unknown terms which can be obtained by satisfying the boundary conditions in the edges. Deriving the values of $\{K_1\}$ and $\{K_2\}$ gives the displacement field of the cylinder. Thus the inter-laminar stresses are obtained. In this part the free boundary condition is analysed.

For free edges at $x = L$ or $x = -L$, the boundary conditions include satisfaction of following $3(N + 1)$ equations as

$$\begin{matrix} M_{x\theta}^i = 0 \\ R_x^i = 0 \\ M_x^i = 0 \end{matrix} \qquad i = 1, \ldots, N + 1 \tag{28}$$

Imposing the boundary conditions at $x = L$ and $x = -L$, include satisfaction of $6(N + 1)$ equation which will be used for obtaining $6(N + 1)$ unknown constants in $\{K_1\}$ and $\{K_2\}$. If the boundary conditions in both edges at $x = \pm L$ be the same, it can be shown that $\{\eta\}$ would be an odd function and $\{\xi\}$ would be an even function of x, and so it can be concluded that $\{K_2\} = \{0\}$. In this case the unknown constant of $\{K_1\}$ can be obtained by imposing the boundary conditions on one of the edges at $x = L$ or $x = -L$. For example the free boundary condition at $x = L$ can be imposed to the equations as

$$\begin{gathered} [\mathrm{P}_1][U][\mathrm{Cos}h(\lambda L)]\{\mathrm{K}_1\} = [P_1][B]^{-1}\{F\} \\ [\mathrm{P}_2][U][\mathrm{Cos}h(\lambda L)]\{\mathrm{K}_1\} = [P_2][B]^{-1}\{F\} \\ [P_3][B][U][\sinh(\lambda L)]\{\mathrm{K}_1\} = \{0\} \end{gathered} \tag{29}$$

In which

$$[P_1] = \left[D_{11}^{ij} \quad D_{16}^{ij} \quad \left(B_{13}^{ij} + \frac{1}{R} D_{12}^{ij} \right) \right]$$
$$[P_2] = \left[D_{16}^{ij} \quad D_{66}^{ij} \quad \left(B_{36}^{ij} + \frac{1}{R} D_{26}^{ij} \right) \right] \tag{30}$$
$$[P_3] = \left[B_{55}^{ij} \quad \left(B_{45}^{ij} - \frac{1}{R} D_{45}^{ij} \right) \quad D_{55}^{ij} \right]$$

3. Results and discussion

To investigate the inter-laminar stresses in the rotating laminated cylindrical shells, in this part, the inter-laminar normal and shear stresses are presented for various laminated cylinders. The Layerwise theory formulation that discussed in the previous part is used to determine the inter-laminar stresses. The laminated cylinder which is made of graphite-epoxy lamina is studied. The mechanical properties of graphite-epoxy lamina are given in Table 1.

In a homogenous and isotropic thin rotating cylinder, the circumferential stress can be obtained as $\sigma_\theta = \rho R^2 \omega^2$ in which ρ is the mass density and ω (rad/s) is the angular velocity of the rotation and R is the mean radius of cylinder. In this study, the dimensionless stresses σ^* are defined as

$$\sigma^* = \frac{\sigma}{\rho R^2 \omega^2} \tag{31}$$

The mean radius of the cylinder is taken as R = 30 mm, R/h = 30, $L = 2h$ and ω = 200 Hz. The convergence of the inter-laminar normal stress σ_z at $[90°/0°]_s$ cylinder at the interface of physical layers at the free edge is studied in this Fig. 2. Each physical layer is divided in to n_p numerical

Table 1 Mechanical properties laminated cylindrical shell (Byron Pipes and Pagano 1970)

	E_1 (Gpa)	E_2 (Gpa)	E_3 (Gpa)	ν_{12}	ν_{23}	ν_{13}	G_{12}(Gpa)	G_{23}(Gpa)	G_{13}(Gpa)
Graphite-Epoxy	137.9	14.48	14.48	0.21	0.21	0.21	5.86	5.86	5.86

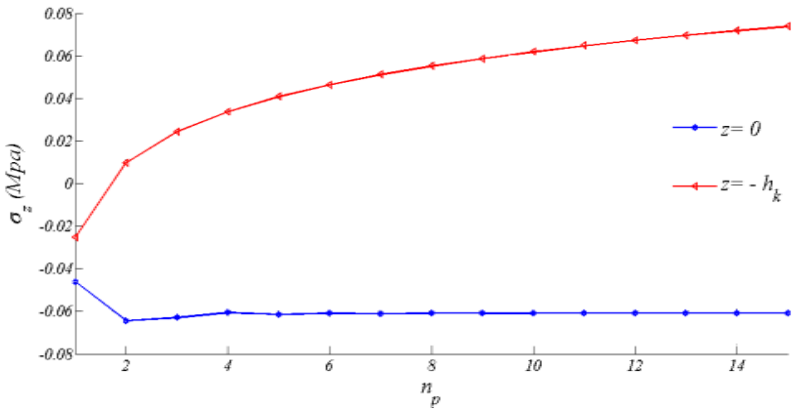

Fig. 2 Distribution of inter-laminar stress σ_z versus number of mathematical layers of each physical layer of $[90°/0°]_s$ cylindrical shell (at $x = L$)

layer and the total number of numerical layer is $N = p \times n_p$ where p is the number of physical layers. Fig. 2, shows normal stress σ_z versus number of numerical (mathematical) layers of each physical layer (n_p) of laminated composite in two interfaces of 0°/0° and 0°/90° at the edge $x = L$.

It can be seen that the inter-laminar normal stress σ_z at the interface of 0°/0° ($z = 0$) is converged for $n_p > 7$. The inter-laminar normal stress σ_z does not converge and increases by increasing the number of mathematical layers in interface of 0°/90° ($z = h_k$). Because of the difference of stacking of laminates, singularity of inter-laminar stresses happen in vicinity of intersection of interfaces of laminates and stress is not converged. So, very large amount of Inter-laminar stress occurs in free edges and intersection of interfaces of two laminate with different fiber orientations or different mechanical properties. Some researchers (Icardi and Bertetto 1995, Kassapoglou and Lagace 1986, Raju and Crews 1981, Kant and Swaminathan 2000 and Kim and Hong 1991) reported existence of singularity of inter-laminar normal stress at the free edge at the interface of 0°/90° layers in which the physical properties of adjacent layers are different. In this study, the number of numerical layers of each physical layer are assumed as $n_p = 10$.

To validate the results, first, the Layerwise theory is used for a symmetric $[90°/0°]_s$ laminated cylindrical shell and compared with those obtained from finite-element solution. For modeling the laminated cylindrical shell in ANSYS, because of the axisymmetric conditions in loading and boundary conditions of the rotating cylindrical shell, the element type of axisymmetric solid 186 is used. The meshing of the model is mapped and fine. Number of elements at length and thickness of the laminated composite shell respectively are 200 and 240 elements. Angular velocity is applied on composite shell. The mechanical properties of layers are as same as the properties used in LWT. The layer stacking of model is cross-ply $[90°/0°]_s$. In the model of FEM with lower numbers of elements the results of inter-laminar stresses are not exact. It is obvious that the number of elements in FEM is much more than number of layers in LWT.

All the obtained results show a good agreement between LWT and FEM. The results of the inter-laminar stress σ_z^* along 90°/0° interface ($z = h_k$) of $[90°/0°]_s$ cylindrical shell with free edges are compared in Fig. 3. The comparison of Layerwise theory and finite element method shows a well agreement between the results. As it is expected, the inter-laminar stress σ_z^* increases suddenly near the vicinity of the free edge.

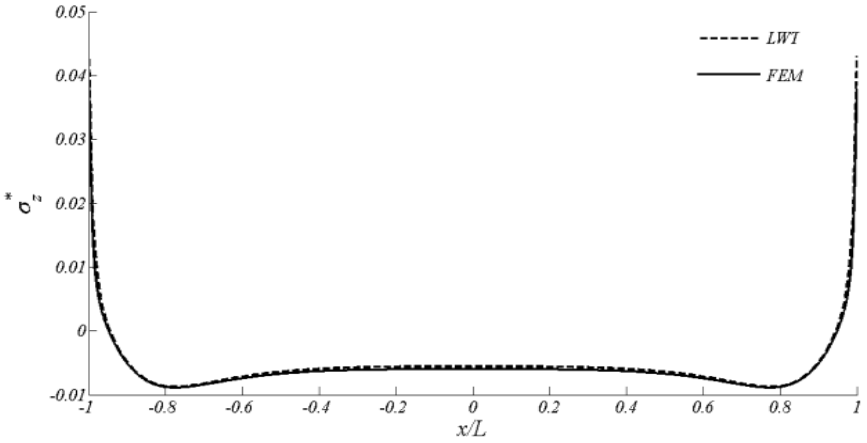

Fig. 3 The comparison of the results of LWT, FEM for σ_z^* along the interface of the $[90°/0°]_s$ laminated cylindrical shell (at $z = h_k$)

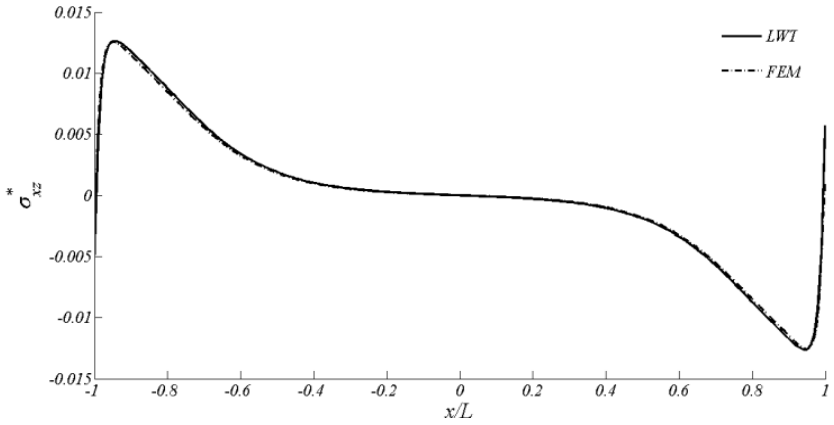

Fig. 4 The comparison between results of LWT and FEM for σ^*_{xz} along the interface of the $[90°/0°]_s$ laminated cylindrical shell (at $z = h_k$)

It can be seen in Fig. 4 that the transverse shear stress σ^*_{xz} increases then decreases near the free edge. The accuracy of results of Layerwise theory is validated comparing with FEM results. Also Figs. 5 and 6 shows through the thickness stresses of σ^*_z and σ^*_{xz} near the free edge of laminated cylindrical shell at $x = 0.99L$ in symmetric laminated cylinder with layer stacking of $[90°/0°]_s$. It is obvious that the results of LWT are in a good agreement with the results of FEM. As it was expected inter-laminar stress σ^*_z is equal to zero at bottom and top surfaces which are the free condition surfaces of laminated cylindrical shell. According to Fig. 6 the maximum inter-laminar stress is not occur exactly at the interface of laminated cylindrical shell. The value of σ^*_{xz} changes in the interface of physical layers.

The distribution of the inter-laminar normal stress σ^*_z at the interfaces of $[90°/0°]_s$ cylindrical shell ($z = h_k$, $z = -h_k$ and $z = 0$) is shown in Fig. 7. It is observed that the normal inter-laminar stress

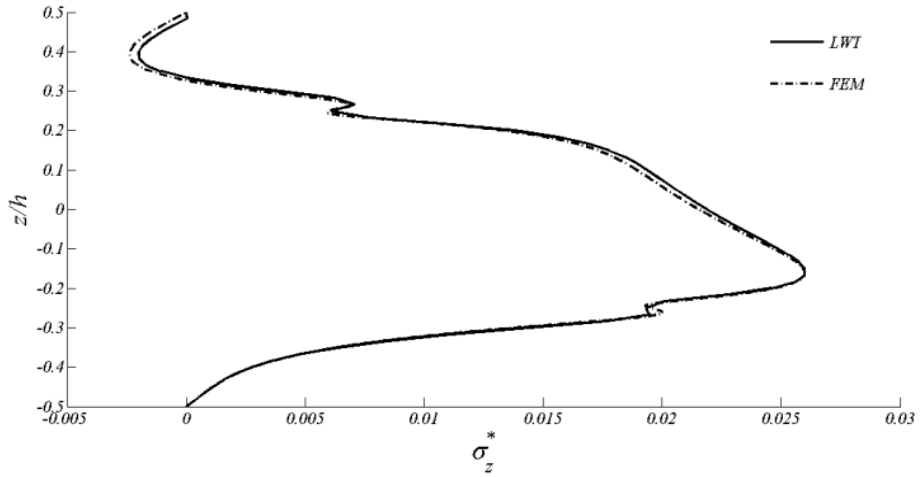

Fig. 5 The comparison between results of LWT and FEM for σ^*_z through the thickness of the $[90°/0°]_s$ laminated cylindrical shell at $x = 0.98L$

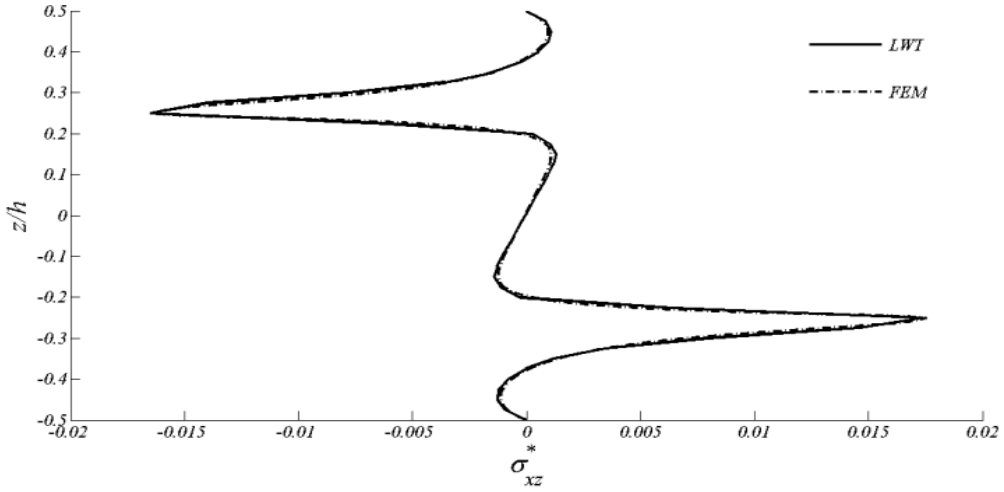

Fig. 6 The comparison between results of LWT and FEM for σ^*_{xz} through the thickness of the $[90°/0°]_s$ laminated cylindrical shell at $x = 0.98L$

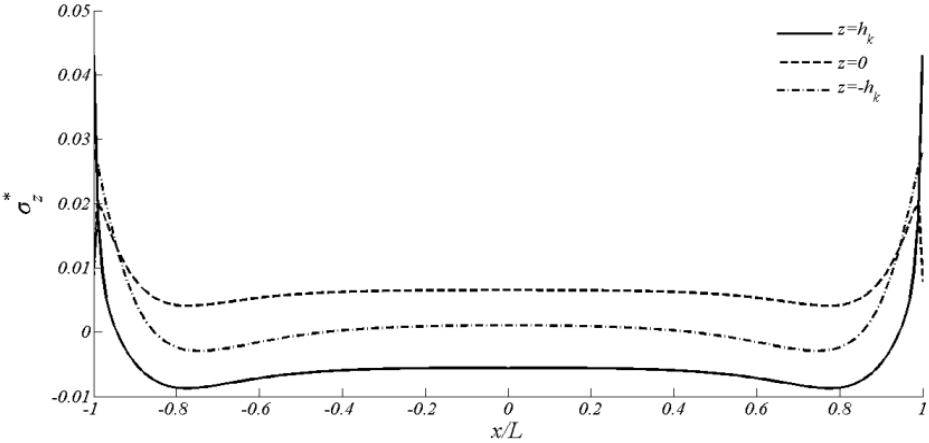

Fig. 7 Distribution of inter-laminar stress σ^*_z along the interfaces of the $[90°/0°]_s$ cylindrical shell (at $z = h_k$, $z = -h_k$ and $z = 0$)

σ^*_z alters significantly at the vicinity of the free edge. σ^*_z is positive in both $z = h_k$ and $z = -h_k$ while it is negative at $z = 0$ near the free edge.

The distribution of the inter-laminar shear stress σ^*_{xz} along the interface of physical layers of $[90°/0°]_s$ cylindrical is shown in Fig. 8. It is observed that σ^*_{xz} rises near the free edges because of the free edge effect. The amount of σ^*_{xz} at $z = h_k$ and $z = -h_k$ are equal with opposite signs. It is shown that σ^*_{xz} is equal to zero in the middle of cylindrical shell.

The trend of change of inter-laminar stress σ^*_z across the thickness of cross-ply laminated cylindrical shell is shown in Fig. 9. It is seen that the distribution of the inter-laminar stress σ^*_z dependes on the orientation of ply. This stress varies suddenly at the interface of layers with different physical properties. The maximum amount of σ^*_z occurs near the free edge ($x = 0.98L$).

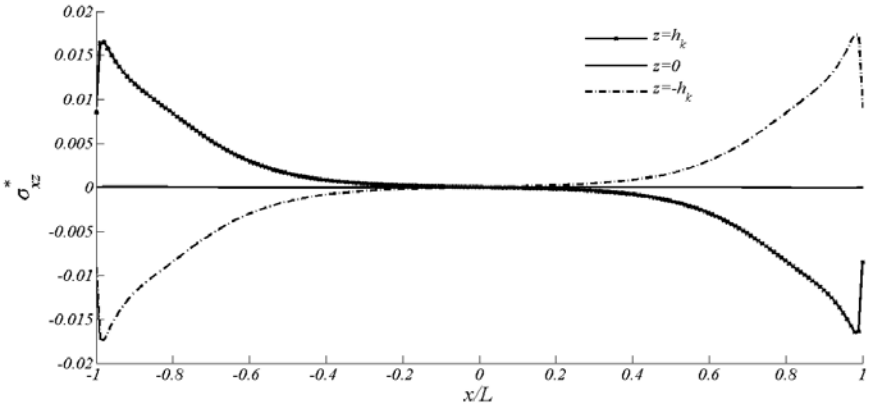

Fig. 8 Distribution of inter-laminar stress σ_{xz}^{*} along the interfaces of $[90°/0°]_s$ cylindrical shell (at $z = h_k$, $z = -h_k$ and $z = 0$)

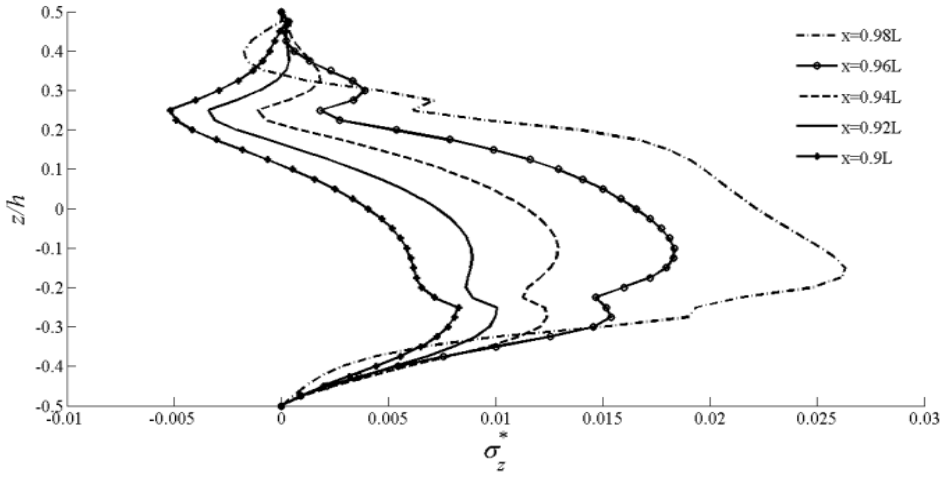

Fig. 9 Through the thickness distribution of inter-laminar stress σ_{z}^{*} at the vicinity of edges of $[90°/0°]_s$ cylindrical shell

The distribution of inter-laminar stress $\sigma_z{}^{*}$ along the physical interfaces $z = -h_k$, $z = 0$ and $z = h_k$ in [90°/0°/90°/0°] cylindrical shell with free boundary conditions at both edges is shown in Fig. 10. Comparing this Figure with Fig. 7 shows the difference between the distributions of inter-laminar normal stress in [90°/0°/90°/0°] and $[90°/0°]_s$ cylinders.

The distribution of inter-laminar shear stress σ_{xz}^{*} at the interface of physical layers of un-symmetric [90°/0°/90°/0°] cylinder with free boundary condition is shown in Fig. 11. It shows that the amount of inter-laminar shear stress σ_{xz}^{*} at $z = h_k$ is higher than $z = -h_k$. The layer stacking is also effective in amount of inter-laminar stresses, which is obvious by comparing Figs. 11 and 4.

Distribution of inter-laminar shear stress σ_{xz}^{*} along the interfaces of physical layers of $[0°/90°]_s$ cylinder with free boundary condition is shown in Fig. 12. It is observed that σ_{xz}^{*} rises near the free edges because of edge effect. Comparing Fig. 12 with Fig. 8, it is obvious that σ_{xz}^{*} in $[0/90]_s$ is equal to $[90/0]_s$ with opposite signs in all physical interfaces.

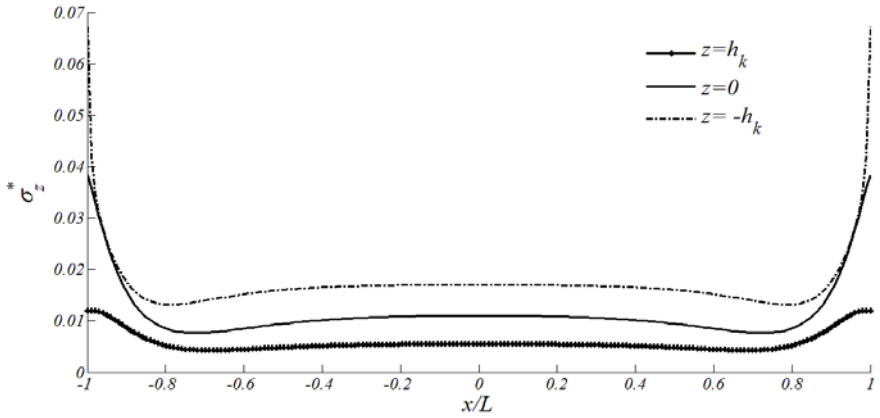

Fig. 10 Distribution of inter-laminar stress σ_z^* of a [90°/0°/90°/0°] cylindrical shell

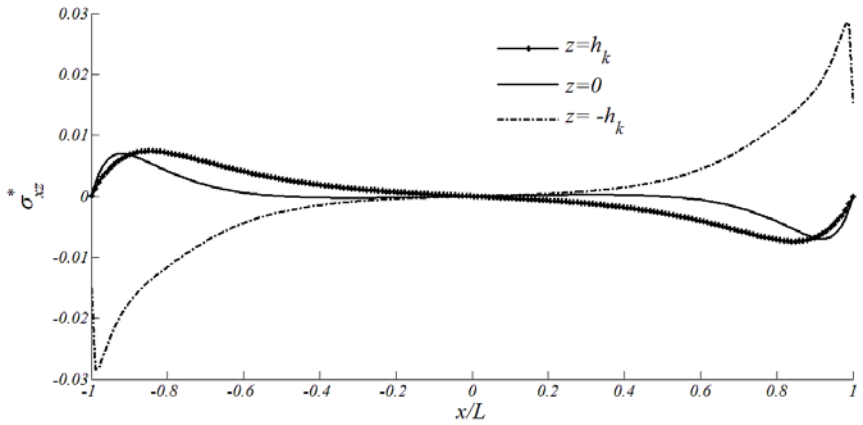

Fig. 11 Distribution of inter-laminar stress σ_{xz}^* along the interfaces of [90°/0°/90°/0°] cylindrical shell

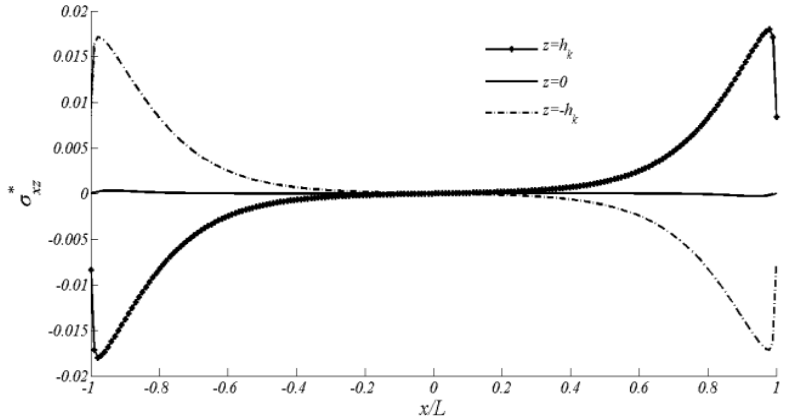

Fig. 12 Distribution of inter-laminar stress σ_{xz}^* along the $[0°/90°]_s$ cylindrical shell (at $z = h_k$, $z = -h_k$ and $z = 0$)

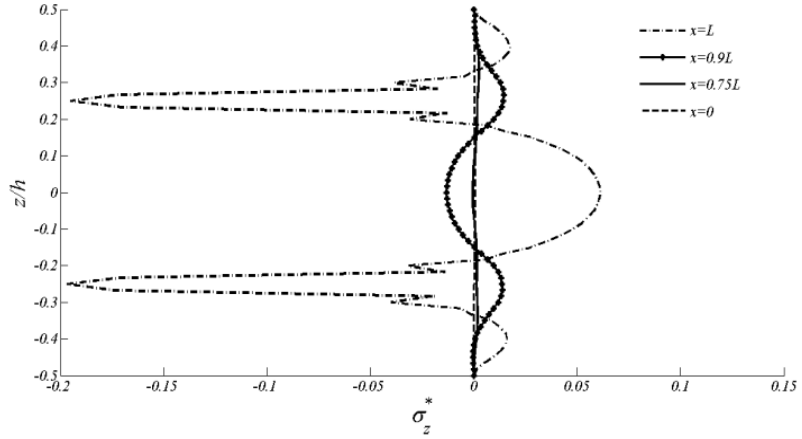

Fig. 13 The Distribution of inter-laminar stress σ_z^* versus thickness of the $[\pm 45°]_s$ cylindrical shell

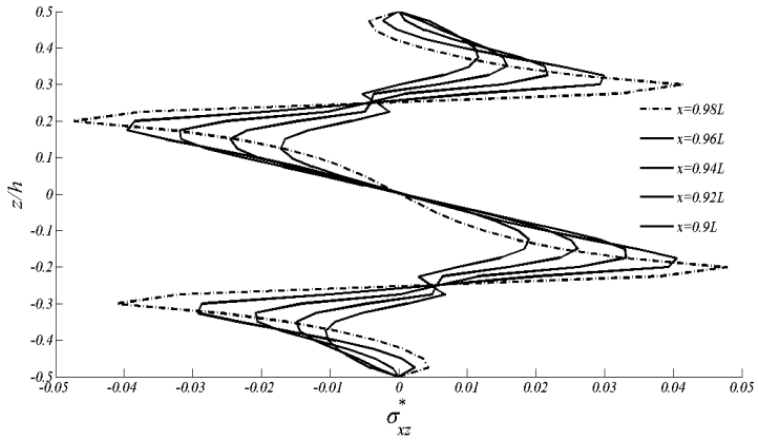

Fig. 14 Distribution of inter-laminar stress σ_{xz}^* versus thickness of the $[\pm 45°]_s$ cylindrical shell

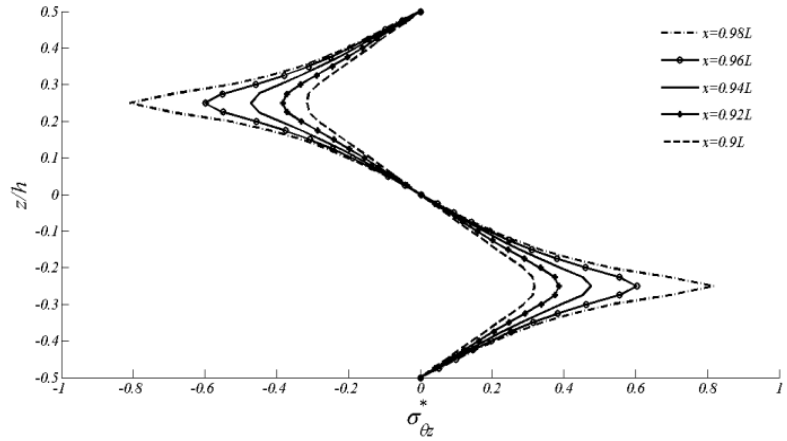

Fig. 15 Distribution of inter-laminar stress $\sigma_{\theta z}^*$ versus thickness of the $[\pm 45°]_s$ cylindrical shell

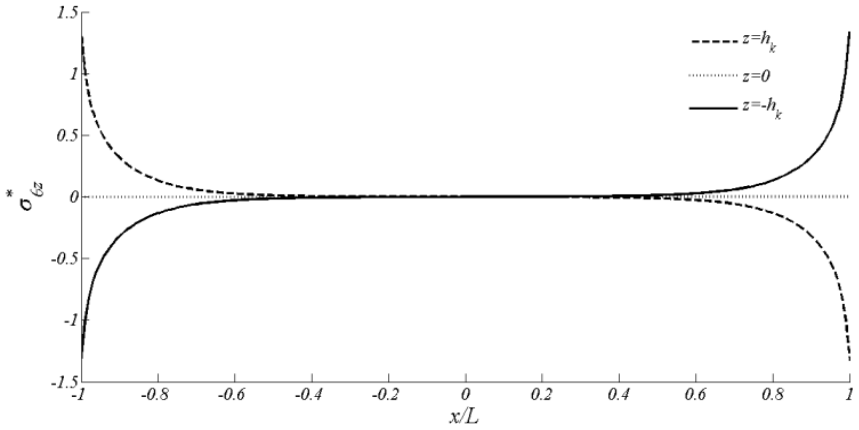

Fig. 16 Distribution of inter-laminar stress $\sigma^*_{\theta z}$ along the interfaces of $[\pm 45°]_s$ cylindrical shell

The distribution of inter-laminar normal stress σ^*_z and shear stresses σ^*_{xz} and $\sigma^*_{\theta z}$ through the thickness of $[\pm 45]_s$ cylindrical shell at various lengths are respectively illustrated in Figs. 13-15. It is distinctively clear that, the amount of inter-laminar stresses differs suddenly at the interface. The maximum point of inter-laminar stress σ^*_z occurs near the free edge because of the edge effect.

Fig. 16 indicates the distribution of inter-laminar stress $\sigma^*_{\theta z}$ at the top and bottom, physical interfaces ($z = h_k$ and $z = -h_k$) of laminated composite. The amount of inter-laminar stress is equal at top and bottom interfaces with different signs and is equal to zero in middle surface of composite. $\sigma^*_{\theta z}$ is positive at $z = h_k$ at $x = -L$ to $x = 0$ at $x = 0$ it is equal to zero then from $x = 0$ to $x = L$ it becomes negative.

Distribution of σ^*_z along the interface of $[\pm 45]_s$ at $z = \pm h_k$ and $z = 0$ is shown in Fig. 17. Inter-laminar stresses of σ^*_z alter in the vicinity of free edge. It is obvious that changing the layer stacking of the composite may control the amount of rise of inter-laminar stress at the free edge. σ^*_z is zero at the middle of interfaces while, it rises near the free edge. Normal inter-laminar stress σ^*_z is positive at $z = 0$ while it is negative in both $z = h_k$ and $z = -h_k$.

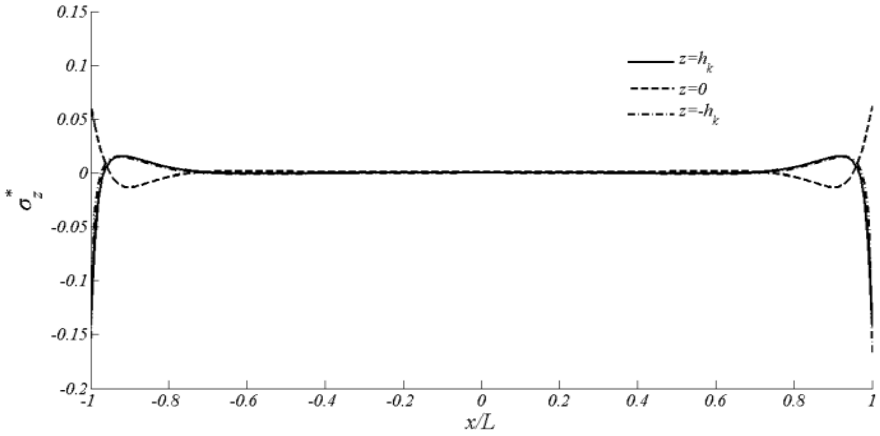

Fig. 17 Distribution of inter-laminar stress σ^*_z along the interfaces of $[\pm 45°]_s$ cylindrical shell

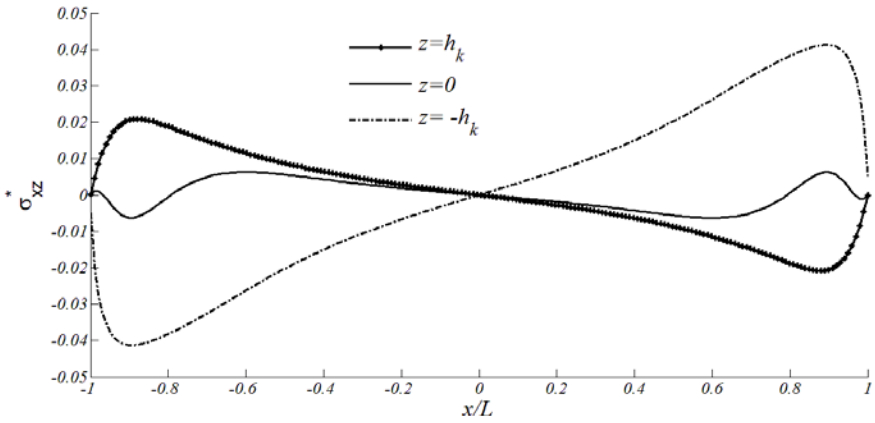

Fig. 18 Distribution of inter-laminar stress σ_{xz}^{*} along the interfaces of [-45°/45°/-45°/45°] cylindrical shell

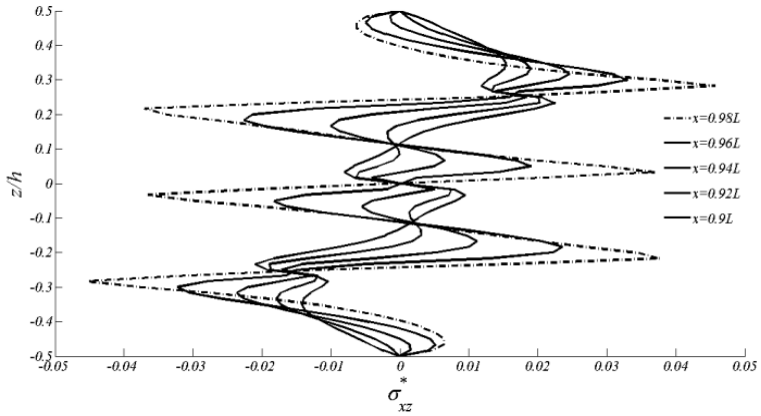

Fig. 19 Distribution of inter-laminar stress σ_{xz}^{*} of [-45°/45°/-45°/45°] cylindrical shell across the thickness

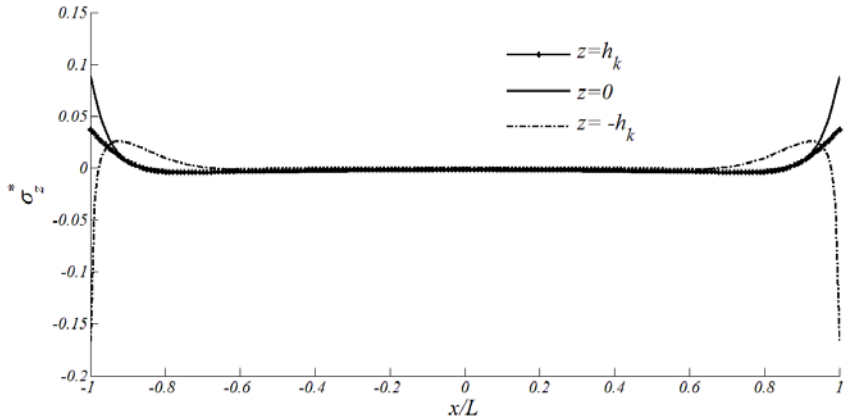

Fig. 20 Distribution of inter-laminar stress σ_{z}^{*} along the [-45°/45°/–45°/45°] cylindrical shell

Distribution of σ_{xz}^* along the length of the [-45°/45°/-45°/45°] cylinder at various interfaces and across the thickness of it is illustrated respectively in Figs. 18 and 19. As it is seen the inter-laminar stress increases in anti-symmetric layups.

The distribution of σ_{xz}^* along the length of un-symmetric [-45°/45°/-45°/45°] cylindrical shell with free boundary condition is shown in Fig. 20. Interlaminar normal stress is compressive in the free edge at $z = -h_k$ and is tensile at $z = 0$ and $z = h_k$. As seen the Interlaminar normal stress vanishes far from the edges.

The inter-laminar shear stress $\sigma_{\theta z}^*$ along the [-45°/45°/-45°/45°] un-symmetric cylindrical is presented in Fig. 21. It is seen that $\sigma_{\theta z}^*$ at $z= -h_k$ is lower in comparison to $\sigma_{\theta z}^*$ at $z= h_k$..

Fig. 22 shows the effect of speed of rotation of cylindrical shell on the distribution of inter-laminar stress σ_z^*. It is clear that higher speed of rotation of laminated composite causes higher changes of inter-laminar stress at the free edge.

The effect of radius to thickness ratio of cylinder on the distribution of inter-laminar normal stress σ_z^* is analyzed in Fig. 24. The radius of the cylinder is considered as constant and the

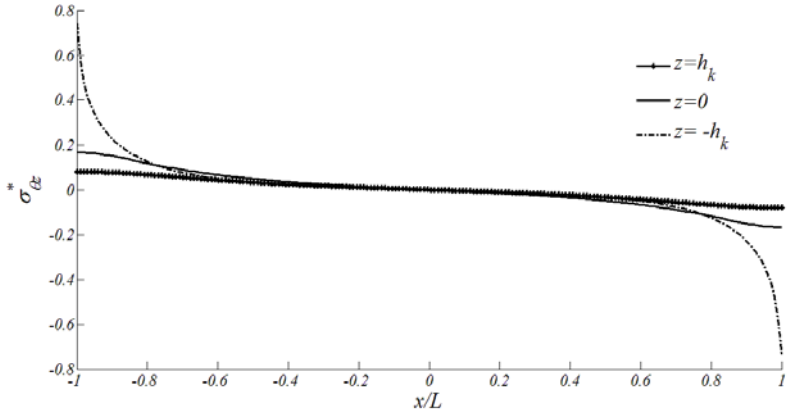

Fig. 21 Distribution of inter-laminar stress $\sigma_{\theta z}^*$ of the [-45°/45°/-45°/-45°] cylindrical shell

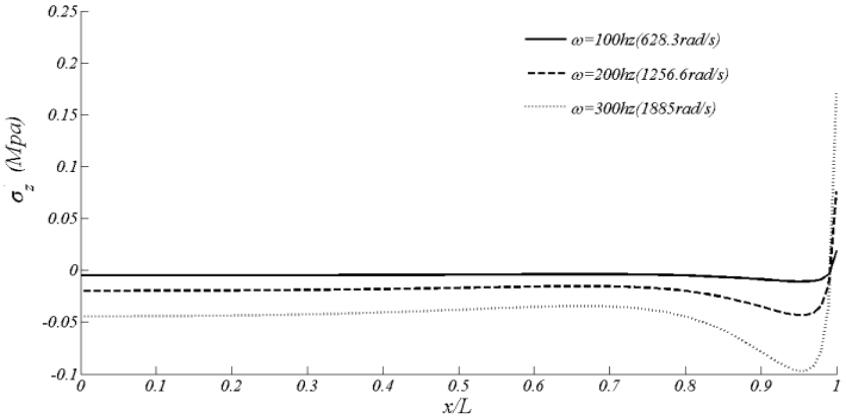

Fig. 22 The effect of speed of rotation of laminated cylindrical shell on distribution of inter-laminar stress σ_z^* along the $[0°/90°]_s$ cylindrical shell (at $z = -h_k$)

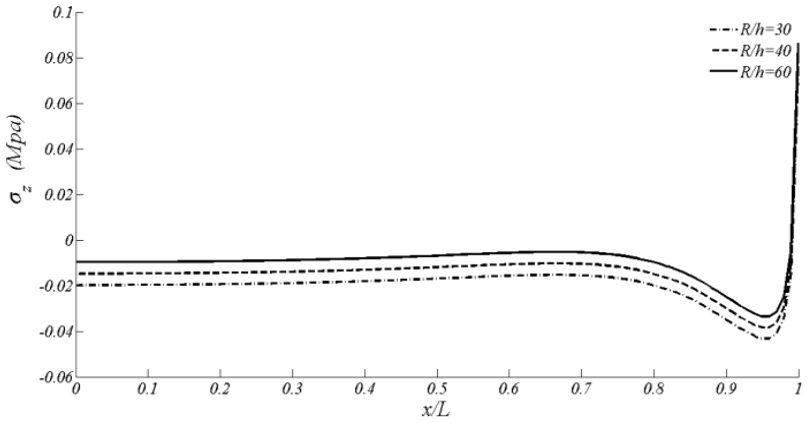

Fig. 23 The effect of radius to thickness ratio of $[0°/90°]_s$ cylindrical shell on the distribution of inter-laminar stress σ_z^* along the cylindrical shell(at $z = -h_k$)

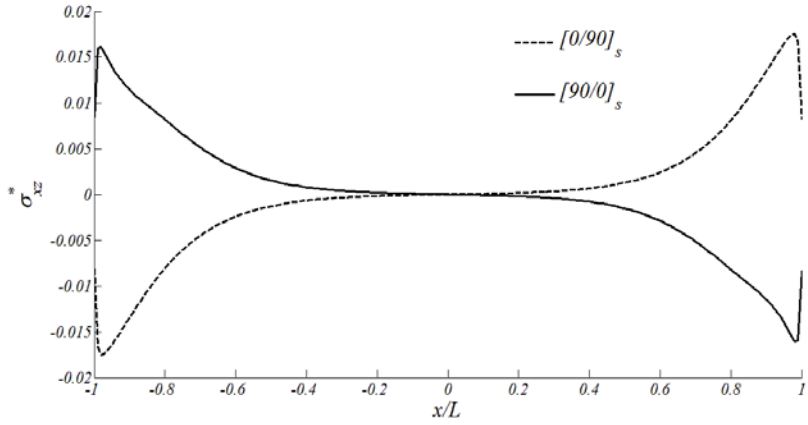

Fig. 24 Distribution of inter-laminar stress σ_{xz}^* along $[0°/90°]_s$ and $[90°/0°]_s$ cylindrical shell (at $z = -h_k$)

thickness is changed. It is obvious that lower ratio of radius to thickness causes higher inter-laminar stress at the vicinity of free edge.

Fig. 25 compares inter-laminar shear stress σ_{xz}^* at $z = h_k$ in $[90°/0°]_s$ and $[0°/90°]_s$ cylinders. It is shown that σ_{xz}^* alters near the free edge in both layer stacking. Interlaminar stress σ_{xz}^* is equal with different signs in both cylindrical shells.

4. Conclusions

In this study the Layerwise theory formulation approach is presented for analysing the inter-laminar and in-plane stresses in the laminated thin composite cylinder with arbitrary layer stacking which is subjected to rotational body force. Unlike the classical and first order shear deformation theories, the Layerwise theory of Reddy is capable to investigate three dimensional stresses. Therefore, it is used to formulate the problem. Considering the axisymmetric conditions of the

problem, a general displacement field is assumed which includes the circumferential displacement. The equations of motion are derived as a function of displacement field. To solve the governing equations, the state-space variables are defined and the solution of the governing equations is obtained for the free boundary condition and the displacement and stress fields are obtained. To validate the LWT, a comparison is done between the results of the FEM and the LWT. Although the number of equations used in LWT is significantly lower than the equations used in FEM, but the numerical results of LWT show an excellent agreement with the results of FEM. The numerical results for in-plane and inter-laminar stresses are presented for the free boundary condition and for various symmetric or anti-symmetric layer stacking. It is seen that the inter-laminar stresses varies suddenly in the vicinity of the edges and can cause delamination and local damage near the edges of rotating laminated cylinders.

References

Afshin, M., Sadighi, M. and Shakeri, M. (2010), "Free-edge effects in a cylindrical sandwich panel with a flexible core and laminated composite face sheets", *Mech. Compos. Mater.*, **46**(5), 539-554.

Ahmadi, I. (2016), "Edge stresses analysis in thick composite panels subjected to axial loading using layerwise formulation", *Struct. Eng. Mech., Int. J.*, **57**(4), 733-762.

Alankaya, V. and Oktem, A.S. (2016), "Static analysis of laminated and sandwich composite doubly-curved shallow shells", *Steel Compos. Struct., Int. J.*, **20**(5), 1043-1066.

Asgari, M. and Akhlaghi, M. (2011), "Thermo-mechanical analysis of 2d-fgm thick hollow cylinder using graded finite elements", *Adv. Struct. Eng.*, **14**(6), 1059-1073.

Başar, Y., Itskov, M. and Eckstein, A. (2000), "Composite laminates: nonlinear interlaminar stress analysis by multi-layer shell elements", *Comput. Method. Mech. Eng.*, **185**(2), 367-397.

Byron Pipes, R. and Pagano, N.J. (1970), "Interlaminar stresses in composite laminates under uniform axial extension", *J. Compos. Mater.*, **4**(4), 538-548.

Ealias, J., Lalmoni, J.J.M. and Mattam, J.J. (2013), "Study of inter-laminar shear stress of composite structures", *Int. J. Emerg. Technol. Adv. Eng.*, **3**(8), 543-552.

Edfawy, E. (2016), "Thermal stresses in a non-homogeneous orthotropic infinite cylinder", *Struct. Eng. Mech, Int. J.*, **59**(5), 841-852.

Goswami, S. and Becker, W. (2016), "Analysis of sandwich plates with compressible core using layerwise refined plate theory and interface stress continuity", *J. Compos. Mater.*, **50**(2), 201-217.

Hayashi, T. (1967), "Analytical study of interlaminar shear stresses in a laminated composite", *Trans. Japan Soc. Aeronaut. Eng. Space Sci.*, **10**(17), 43-48.

Hosseini Kordkheili, S.A. and Naghdabadi, R. (2007), "Thermoelastic analysis of functionally graded cylinders under axial loading", *J. Therm. Stress.*, **31**(1), 1-17.

Icardi, U. and Bertetto, A.M. (1995), "An evaluation of the influence of geometry and of material properties at free edges and at corners of composite laminates", *Comput. Struct.*, **57**(4), 555-571.

Javed, S., Viswanathan, K.K. and Aziz, Z.A. (2016), "Free vibration analysis of composite cylindrical shells with non-uniform thickness walls", *Steel Compos. Struct., Int. J.*, **20**(5), 1087-1102.

Kant, T. and Swaminathan, K. (2000), "Estimation of transverse/interlaminar stresses in laminated composites–a selective review and survey of current developments", *Compos. Struct.*, **49**(1), 65-75.

Kapoor, H., Kapania, R.K. and Soni, S.R. (2013), "Interlaminar stress calculation in composite and sandwich plates in NURBS isogeometric finite element analysis", *Compos. Struct.*, **106**, 537-548.

Kassapoglou, C. and Lagace, P.A. (1986), "An efficient method for the calculation of interlaminar stresses in composite materials", *J. Appl. Mech.*, **53**(4), 744-750.

Kassegne, S.K. and Reddy, J.N. (1998), "Local behavior of discretely stiffened composite plates and cylindrical shells", *Compos. Struct.*, **41**(1), 13-26.

Khandelwal, R.P. and Chakrabarti, A. (2015), "Calculation of interlaminar shear stresses in laminated shallow shell panel using refined higher order shear deformation theory", *Compos. Struct.*, **124**, 272-282.
Kim, J.Y. and Hong, C.S. (1991), "Three-dimensional finite element analysis of interlaminar stresses in thick composite laminates", *Comput. Struct.*, **40**(6), 1395-1404.
Levy, S. and Tang, A. (1975), "A boundary layer theory – Part II: Extension of laminated finite strip", *J. Compos. Mater.*, **9**(1), 42-52.
Madhukar, S. and Singha, M.K. (2013), "Geometrically nonlinear finite element analysis of sandwich plates using normal deformation theory", *Compos. Struct.*, **97**, 84-90.
Mantari, J.L., Oktem, A.S. and Guedes Soares, C. (2012), "A new trigonometric layerwise shear deformation theory for the finite element analysis of laminated composite and sandwich plates", *Comput. Struct.*, **94**, 45-53.
Matsunaga, H. (2009), "Stress analysis of functionally graded plates subjected to thermal and mechanical loadings", *Compos. Struct.*, **87**(4), 344-357.
Maturi, D.A., Ferreira, A.J.M., Zenkour, A.M. and Mashat, D.S. (2014), "Analysis of sandwich plates with a new layerwise formulation", *Composites: Part B*, **56**, 484-489.
Miri, A.K. and Nosier, A. (2011), "Out-of-plane stresses in composite shell panels: Layerwise and elasticity solutions", *Acta Mech.*, **220**(1-4), 15-32.
Pagano, N.J. (1974), "On the calculation of interlaminar normal stress in composite laminate", *J. Compos. Mater.*, **8**, 65-81.
Pagano, N.J. and Pipes, R.B. (1974), "Interlaminar stresses in composite kaminates, An approximate elasticity solution", *J. Appl. Mech.*, **41**, 668-672.
Plagianakos, T.S. and Sarvanos, D.A. (2009), "Higher-order layerwise laminate theory for the prediction of inter-laminar shear stresses in thick composite and sandwich composite plates", *Compos. Struct.*, **87**(1), 23-35.
Puppo, A.H. and Evensen, H.A. (1970), "Interlaminar shear in laminated composites under generalized plane stress", *J. Compos. Mater.*, **4**(2), 204-220.
Raju, I.S. and Crews Jr., J.H. (1981), "Interlaminar stress singularities at a straight free edge in composite laminates", *Comput. Struct.*, **14**(1), 21-28.
Reddy, J.N. (1992), "A layerwise shell theory with applications to buckling and vibration of cross-ply laminated stiffened circular cylindrical shells", Center for Composite Materials and Structures, Virginia Polytechnic Institute State University, **92**.
Varadan, T.K. and Bhaskar, K. (1991), "Bending of laminated orthotropic cylindrical shells—An elasticity approach", *Compos. Struct.*, **17**(2), 141-156.
Vijayakumar, K. (2011), "Layerwise theory of bending of symmetric laminates with isotropic plies", *AIAA J.*, **49**(9), 2073-2076.
Waltz, T.L. and Vinson, J.R. (1976), "Interlaminar stresses in laminated cylindrical shells of composite materials", *AIAA J.*, **14**(9), 1213-1218.
Wang, X., Cai, W. and Yu, Z.Y. (2002), "An analytic method for interlaminar stress in a laminated cylindrical shell", *Mech. Adv. Mater. Struct.*, **9**(2), 119-131.
Whitney, J.M. (1973), "Free-edge effects in the characterization of composite materials", *Am. Soc. Test. Mater.*, **521**, 167-180.
Wu, C-P. and Chi, Y-W, (1999), "Asymptotic solutions of laminated composite shallow shells with various boundary conditions", *Acta Mechanica*, **132**(1-4), 1-18.
Yang, C., Chen, J. and Zhao, S. (2013), "The interlaminar stress of laminated composite under uniform axial deformation", *MNSMS*, **3**(2), 49-60.
Yas, M.H., Shakeri, M., Heshmati, M. and Mohammadi, S. (2011), "Layerwise finite element analysis of functionally graded cylindrical shell under dynamic load", *J. Mech. Sci. Technol.*, **25**(3), 597-604.

CC